A Hybrid Method for the Calculation of the Resistance and Inductance of Transmission Lines with Arbitrary Cross Sections

Michael J. Tsuk, *Member, IEEE*, and Jin Au Kong, *Fellow, IEEE*

Abstract—**The frequency-dependent resistance and inductance of uniform transmission lines are calculated with a hybrid technique that combines a cross-section coupled circuit method with a surface integral equation approach. The coupled circuit approach is most applicable for low-frequency calculations, while the integral equation approach is best for high frequencies. The low-frequency method consists in subdividing the cross section of each conductor into triangular filaments, each with an assumed uniform current distribution. The resistance and mutual inductance between the filaments are calculated, and a matrix is inverted to give the overall resistance and inductance of the conductors. The high-frequency method expresses the resistance and inductance of each conductor in terms of the current at the surface of that conductor and the derivative of that current normal to the surface. A coupled integral equation is then derived to relate these quantities through the diffusion equation inside the conductors and Laplace's equation outside. The method of moments with pulse basis functions is used to solve the integral equations. An interpolation between the results of these two methods gives very good results over the entire frequency range, even when few basis functions are used. Results for a variety of configurations are shown and are compared with experimental data and other numerical techniques.**

I. Introduction

With the ever-increasing speed and density of modern integrated circuits, the need for electromagnetic wave analysis of phenomena such as the propagation of transient signals, especially the distortion of signal pulses, becomes crucial. One of the most important causes of pulse distortion is the frequency dependence of conductor loss, which can be incorporated into circuit models for transmission lines as frequency-dependent resistance and inductance per unit length. Experimental work measuring the resistance and inductance of conductors has concentrated on circular and rectangular cross sections. Kennelly *et al.* [1] did a thorough experimental study, which was extended to higher frequencies by Kennelly and Affel [2]. Haefner's 1937 paper [3] represents the most extensive experimental data on the resistance of rectangular conductors with a wide variety of width-to-thickness ratios. More recently, Weeks *et al.* [4] did similar work as part of a theoretical treatment of the problem.

In terms of theoretical work, the circular conductor was the first case considered, since it allows an analytical solution. Maxwell [5] examined nonperiodic current; Kelvin [6] solved the periodic case. Carson [7] gave a series solution for the two-wire proximity effect. Cockcroft [8] used the Schwarz–Christoffel transformation to obtain a high-frequency approximation to the skin effect which was expressed in terms of elliptic integrals. Wheeler [9] discussed the "incremental inductance" rule, which is a high-frequency estimate of both the skin and proximity effects. More recently, Casimir and Ubbink [10], [11] presented an overview and summary of the basics of the skin effect, with formulas for the high-frequency limits of simple cases.

In the "filament technique," the conductor (usually rectangular) is divided into a large number of rectangular filaments, which are considered to have uniform current distribution within them. Graneau [12] uses a power-series approach in frequency, which Weeks *et al.* [4] dispensed with. Silvester expands the current in a flat conductor [13] in a series of eigenmodes and the current in a conductor of arbitrary shape [14] in filaments. In both cases he ignores the effect of the placement of the return current, or, in other words, the proximity effect. While these filament methods tend to be very good for low frequencies, since the current density is then almost uniform, they do not model singularities of the current density at high frequencies well.

The other class of methods involves solving the magnetic vector potential integral equation [15]–[21]. The boundary condition is usually on the tangential magnetic field, specified on a closed contour some distance from the conductor. The integral equation is solved by traditional matrix methods, either by expanding the current in a series of orthogonal eigenfunctions [15]–[18] or by dividing the current into subdomain basis functions [19]–[21]. This method is limited in that it requires knowledge of the magnetic field outside the conductor somewhere to

Manuscript received November 21, 1990; revised April 2, 1991. This work was supported by International Business Machines, the Digital Equipment Corporation, RADC under Contract F19628-88-K-0013, the ARO under Contract DAAL03-88-J-0057, the Joint Services Electronics Program under Contract DAAL03-89-C-0001, the ONR under Contract N00014-90-J-1002, and the NSF under Grant 8620029-ECS.

M. J. Tsuk is with the Digital Equipment Corporation, Andover, MA 01810.

J. A. Kong is with the Department of Electrical Engineering and Computer Science, Massachusetts Institute of Technology, Cambridge, MA 02139.

IEEE Log Number 9101028.

calculate the current distribution inside but does not give any general way to determine that field. The more recent work of Cangellaris [22] applies the boundary conditions developed in the filament approaches to the magnetic vector potential integral equation, thus removing one of the principal difficulties of that method; however, it still requires modeling of the current throughout the cross section.

In recent years, new methods have been developed which require modeling the current distribution only on the surface of the wires, rather than throughout the cross section. Djordjević *et al.* [23] assumed a nonphysical distribution of current along the propagation direction, which led to an excess resistance at high frequencies. Their work was modified by Wu and Yang [24] to allow appropriate quasi-TEM propagation. However, since both of these methods depend on the calculation of the normal derivative of the current density, they have numerical difficulties at low frequencies, when the current is almost uniform and the normal derivative is small.

The technique presented in this paper is hybrid cross-section coupled circuit/surface integral equation approach. For low frequencies, a filament method based on the work of Weeks *et al.* is used, except with triangular rather than rectangular patches. For high frequencies, a surface integral equation method is used. However, in contrast to previous work, the calculation of resistance and inductance is based on power dissipation and stored magnetic energy, rather than on impedance ratios. It will therefore be more easily extended to structures where nonuniform propagation can occur. In the middle range of frequency, an interpolation is made between the results of the two methods. Since this is a frequency-domain method, we will assume an $e^{-i\omega t}$ dependence to all quantities.

II. Cross-Section Coupled Circuit Method

For low frequencies, we use a two-dimensional cross-section coupled circuit method to find the resistance and inductance matrices for multiple transmission lines with uniform cross sections. We assume that these transmission lines consist of signal lines over a common return path or "ground plane." The matrices $\bar{\bar{R}}$ and $\bar{\bar{L}}$ are defined by

$$\frac{dV}{dz} = \left(i\omega\bar{\bar{L}} - \bar{\bar{R}}\right)\cdot I \tag{1}$$

where V is the column vector of the voltage differences between the wires and a reference wire (ground plane or return conductor), and I is the column vector of currents flowing in the wires.

Here is an overview of the cross-section coupled circuit method. Each conductor is divided into triangular patches and one of the patches from the return conductor is chosen to be the reference. The current is assumed uniform on the cross section of each patch; in other words, a piecewise-constant approximation to the actual current distribution is used. The resistance and inductance matrices for the patches ($\bar{\bar{r}}$ and $\bar{\bar{l}}$) are then calculated, where these matrices are defined by

$$\frac{dv}{dz} = \left(i\omega\bar{\bar{l}} - \bar{\bar{r}}\right)\cdot \iota \tag{2}$$

where v is the column vector of the voltage differences between the patches and the reference patch, and ι is the column vector of currents flowing in the $\hat{z}$ direction through the patches. There are two conditions on the system: first, that the total current in each wire be the sum of the currents in the patches and, second, that the voltage on each patch in a wire be the same, since no transverse currents are allowed under the quasi-TEM assumption. Using these conditions, the matrices for the patches can be reduced to the matrices for the wires.

For the calculation of $\bar{\bar{r}}$ and $\bar{\bar{l}}$, we follow [4] quite closely. The elements of the resistance matrix of the patches are

$$r_{jk,jk} = \frac{1}{\sigma A_{jk}} + \frac{1}{\sigma A_{00}}$$

$$r_{jk,mn} = \frac{1}{\sigma A_{00}}, \qquad j \neq m, \quad k \neq n \tag{3}$$

where the first subscript indicates the wire, the second the patch within the wire; A_{jk} is the cross-sectional area of patch k on wire j, and patch 0 on wire 0 is the reference of voltage. Also following [4], the elements of the inductance matrix can be written as the sum of partial inductances:

$$l_{jk,mm} = l^{(p)}_{jk,mn} - l^{(p)}_{jk,00} - l^{(p)}_{00,mn} + l^{(p)}_{00,00} \tag{4}$$

where the partial inductances are given by

$$l^{(p)}_{jk,mn} = -\frac{\mu}{4\pi A_{jk} A_{mn}} \int\int dS_{jk} \int\int dS'_{mn} \cdot \ln\left[(x-x')^2 + (y-y')^2\right] \tag{5}$$

where x and y are coordinates on patch jk, and x' and y' are coordinates on patch mn.

In the Weeks method, the patches over which the integrals in (5) are done are rectangles, and the quadruple integral is done quite easily in closed form. However, it is also possible to evaluate the quadruple integral in closed form for any polygonal shapes; the details are rather complex and are left for the Appendix. We therefore use triangular patches as the most flexible means of modeling conductors with arbitrary cross sections; polygons are covered exactly, and we are able to model quite closely other shapes, such as circles.

Once the resistance and inductance matrices for the patches have been obtained, we proceed in the following manner. Taking

$$\frac{dv}{dz} = \left[i\omega\bar{\bar{l}} - \bar{\bar{r}}\right]\cdot \iota \equiv -\bar{\bar{z}}\cdot\iota. \tag{6}$$

The matrix $\bar{\bar{z}}$ is inverted, and $\bar{\bar{y}} = \bar{\bar{z}}^{-1}$. Writing out the

elements of the matrix,

$$I_{jk} = -\sum_{m=0}^{N}\sum_{n=1}^{N_m} y_{jk,mn}\frac{dV_{mn}}{dz} \tag{7}$$

where N is the number of wires and N_m is the number of patches on wire m. The conditions on $\boldsymbol{v}$ and $\boldsymbol{\iota}$ discussed above are applied, to give

$$I_j = -\sum_{m=1}^{N} Y_{jm}\frac{dV_m}{dz} \tag{8}$$

where V and I are the voltage and current column vectors for the wires and where

$$Y_{jm} = \sum_{k=1}^{N_j}\sum_{n=1}^{N_m} y_{jk,mn}. \tag{9}$$

Inverting $\bar{\bar{Y}}$ gives

$$\bar{\bar{Y}}^{-1} = \bar{\bar{R}} - i\omega\bar{\bar{L}}. \tag{10}$$

Thus, the frequency-dependent resistance and inductance matrices for the wires have been obtained.

In [4], the distribution of patches was a function of frequency; as the frequency increased, the patches were concentrated at the edges, where the current is. However, as shall be shown, it is more efficient to switch to a surface integral equation technique for high frequencies; in this paper the distribution of triangular patches is not altered as the frequency is increased. This has the advantage that, since the resistance and inductance matrices of the patches are independent of frequency, $\bar{r}$ and $\bar{l}$ need be calculated only once, no matter for how many frequencies we wish to calculate $\bar{\bar{R}}$ and $\bar{\bar{L}}$.

III. Differential Equations and Boundary Conditions

In this section, the basic equations and boundary conditions which will be used in the surface-integral equation method will be derived. The coordinate system used is shown in Fig. 1. We will rely heavily on quasi-TEM assumptions. First, outside the wires, we assume that the fields are transverse, and that they obey Laplace's equation. In other words, Maxwell's equations outside the wires become

$$\nabla \times \boldsymbol{H} = 0 \tag{11}$$

$$\nabla \cdot \boldsymbol{H} = 0 \tag{12}$$

where ∇ here is only the transverse operator, $\hat{x}\partial/\partial x + \hat{y}\partial/\partial y$. The vector magnetic potential, $\boldsymbol{A}$, is defined such that $\mu\boldsymbol{H} = \nabla \times \boldsymbol{A}$. By the quasi-TEM assumption, $\boldsymbol{J} = \hat{z}J_z$ and $\boldsymbol{A} = \hat{z}A_z$, and it can be shown that

$$\nabla^2 A_z = 0. \tag{13}$$

Also, inside the conductors, the displacement current is ignored; Maxwell's equations become

$$\nabla \times \boldsymbol{E} = i\omega\mu\boldsymbol{H} \tag{14}$$

$$\nabla \times \boldsymbol{H} = \boldsymbol{J} \tag{15}$$

$$\nabla \cdot \boldsymbol{H} = 0. \tag{16}$$

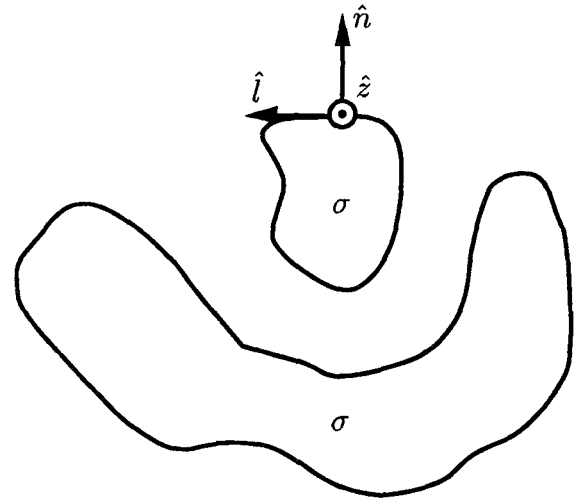

Fig. 1. Coordinate system for surface integral equation method.

Using $\boldsymbol{J} = \sigma\boldsymbol{E}$, this reduces to

$$\nabla^2 J_z + i\omega\mu\sigma J_z = 0. \tag{17}$$

There are two boundary conditions at the interface of the conductors and free space: the continuity of tangential $\boldsymbol{H}$ and of normal $\boldsymbol{B} = \mu\boldsymbol{H}$. If $\boldsymbol{H}$ outside is expressed in terms of A_z, and $\boldsymbol{H}$ inside in terms of J_z, the condition on $\boldsymbol{H}$ reduces to

$$\frac{\partial J_z}{\partial n} = i\omega\sigma\frac{\partial A_z}{\partial n} \tag{18}$$

which is satisfied along all the conductor–free space interfaces. The boundary condition on normal $\boldsymbol{B}$ is more difficult. Assuming that all the materials have the same permeability,

$$\frac{\partial J_z}{\partial l} = i\omega\sigma\frac{\partial A_z}{\partial l}. \tag{19}$$

If the derivatives of two quantities along a line are equal, then those quantities must be equal, to within a constant:

$$J_z = i\omega\sigma\left[A_z - A_q\right]. \tag{20}$$

A_q is constant over a single conductor, but can vary from conductor to conductor.

Finally, it is necessary to be able to specify the total current flowing on a wire. Using Green's first identity,

$$\int\int dS(\phi\nabla^2\psi + \nabla\phi\cdot\nabla\psi) = \oint dl\,\phi\frac{\partial\psi}{\partial n} \tag{21}$$

where dS is a two-dimensional integral over a cross-sectional area, and dl is a one-dimensional integral along the closed contour bounding that area. Also, the normals are defined as pointing out from the region of interest. With $\psi = J_z$ and $\phi = 1$, and considering (17),

$$I = \int\int dS J_z = \frac{i}{\omega\mu\sigma}\int\int dS\,\nabla^2 J_z = \frac{i}{\omega\mu\sigma}\oint dl\frac{\partial J_z}{\partial n} \tag{22}$$

which is an expression for the total current flowing in a

wire in the $\hat{z}$ direction in terms of quantities on the surface.

IV. Determination of Circuit Parameters

Eventually, the quantities of interest are the resistance and inductance per unit length of these conductors. It turns out that it is possible to express these quantities in terms of the current and its normal derivative on the surface of the wires. This is useful, because it means that the problem can be formulated in terms of a set of coupled integral equations involving only these surface quantities, allowing a great savings in computation. The resistances and inductances will be derived through power and energy considerations.

For the resistance, consider a case with a current I flowing in a signal wire and returning in a reference, for example a ground plane. Starting with the power definition of resistance,

$$R=\frac{2P_d}{|I|^2}=\frac{\int\int dS E_z J_z^*}{|\int\int dS J_z|^2}=\frac{1}{\sigma}\frac{\int\int dS|J_z|^2}{|\int\int dS J_z|^2} \tag{23}$$

where the integration in the numerator is over all wires, while that in the denominator is only over the signal wire. The numerator can be put in a more useful form, using (21) with $\phi = J_z$ and $\psi = J_z^*$, and its complex conjugate, together with (17) to get

$$\begin{aligned}\int\int dS|J_z|^2 &= \int\int dS J_z J_z^* \\ &= \frac{1}{2}\frac{i}{\omega\mu\sigma}\int\int dS\left[J_z^*\nabla^2 J_z - J_z\nabla^2 J_z^*\right] \\ &= \frac{1}{2}\frac{i}{\omega\mu\sigma}\oint dl\left[J_z^*\frac{\partial J_z}{\partial n}-J_z\frac{\partial J_z^*}{\partial n}\right] \\ &= \frac{1}{\omega\mu\sigma}\oint dl\,\mathrm{Im}\left\{J_z\frac{\partial J_z^*}{\partial n}\right\}.\end{aligned} \tag{24}$$

Including the total current squared, $|I|^2$, from (22),

$$R=\omega\mu\frac{\oint_{\text{all wires}} dl\,\mathrm{Im}\left\{J_z\frac{\partial J_z^*}{\partial n}\right\}}{\left|\oint_{\text{signal wire}} dl\frac{\partial J_z}{\partial n}\right|^2}. \tag{25}$$

Similarly, starting with a magnetic stored energy definition of inductance per unit length, L:

$$L=\frac{4W_m}{|I|^2}=\mu\frac{\int\int dS\boldsymbol{H}\cdot\boldsymbol{H}^*}{|I|^2} \tag{26}$$

where the range of integration for the numerator is over all space. Using a technique similar to that for (25), combining the contributions from regions inside and outside the wires,

$$L=-\mu\frac{\oint_{\text{all wires}} dl\,\mathrm{Re}\left\{i\omega\sigma A_q\frac{\partial J_z^*}{\partial n}\right\}}{\left|\oint_{\text{signal wire}} dl\frac{\partial J_z}{\partial n}\right|^2}. \tag{27}$$

The mutual resistance and inductance are calculated from energy considerations, and from the self terms calculated above. If we specify a current I_x to flow on line i, and $-I_x$ to flow on line j, we can calculate the power dissipated, P_d, and the stored magnetic energy, W_m, very easily by the above technique. This gives

$$R_{ij}=\frac{1}{2}\left(R_{ii}+R_{jj}-4P_d/I_x^2\right) \tag{28}$$

and

$$L_{ij}=\frac{1}{2}\left(L_{ii}+L_{jj}-8W_m/I_x^2\right). \tag{29}$$

V. Derivation of Coupled Integral Equations

In order to complete the formulation, integral equations are required which relate A_z to $\partial A_z/\partial n$ outside the wires and J_z to $\partial J_z/\partial n$ inside the wires. Starting from Green's theorem:

$$\int\int dS'\left(\phi\nabla^2\psi-\psi\nabla^2\phi\right)=\oint dl'\left(\phi\frac{\partial\psi}{\partial n'}-\psi\frac{\partial\phi}{\partial n'}\right) \tag{30}$$

where the integral dS' is over a cross-sectional region, the integral dl' is over the contour bounding that region, and the normals point out from the region of interest. In general, let $\Psi(\boldsymbol{\rho})$ be either A_z or J_z, where $\boldsymbol{\rho}$ is position in the two-dimensional cross section. Since $\Psi(\boldsymbol{\rho})$ satisfies $\nabla^2\Psi + C\Psi = 0$, where $C = 0$ for Laplace's equation and $C = i\omega\mu\sigma$ for the diffusion equation, a Green's function, $G(\boldsymbol{\rho},\boldsymbol{\rho}')$, can be found which satisfies $\nabla^2 G + CG = -\delta(\boldsymbol{\rho}-\boldsymbol{\rho}')$. Substituting Ψ for ψ and G for ϕ in (30),

$$\begin{aligned}&\int\int dS'\Psi(\boldsymbol{\rho}')\delta(\boldsymbol{\rho}-\boldsymbol{\rho}') \\ &\quad=\oint dl'\left[G(\boldsymbol{\rho},\boldsymbol{\rho}')\frac{\partial\Psi(\boldsymbol{\rho}')}{\partial n'}-\Psi(\boldsymbol{\rho}')\frac{\partial G(\boldsymbol{\rho},\boldsymbol{\rho}')}{\partial n'}\right].\end{aligned} \tag{31}$$

The integral equation will be formulated on the surface, so both $\boldsymbol{\rho}$ and $\boldsymbol{\rho}'$ are on the surface. This places $\delta(\boldsymbol{\rho}-\boldsymbol{\rho}')$ just on the boundary of the dS' integration, and this must be treated carefully. The most straightforward method is that integrating a delta function that lies on the edge of the range of integration gives $1/2$. With this,

$$\begin{aligned}&\oint dl' G(l,l')\frac{\partial\Psi(l')}{\partial n'} \\ &\quad=\oint dl'\Psi(l')\left[\frac{\partial G(l,l')}{\partial n'}+\frac{1}{2}\delta(l-l')\right].\end{aligned} \tag{32}$$

Integral equations for both A_z and J_z can now be

obtained. For the outer equation (13),

$$\oint_{\text{all wires}} dl' G_o(l,l') \frac{\partial A_z(l')}{\partial n'} = \oint_{\text{all wires}} dl' A_z(l') \left[\frac{\partial G_o(l,l')}{\partial n'} - \frac{1}{2}\delta(l-l') \right] \quad (33)$$

where

$$G_o(\boldsymbol{\rho},\boldsymbol{\rho}') = -\frac{1}{2\pi} \ln\left[\sqrt{(x-x')^2+(y-y')^2} \right] \quad (34)$$

and where the sign change in (33) is due to the normals pointing into the region of interest. The range of integration is over the boundary of the free-space region, in other words, over the surface of every wire.

Similarly, for the inner equation (17), for each wire,

$$\oint_{\text{wire } q} dl' G_i(l,l') \frac{\partial J_z(l')}{\partial n'} = \oint_{\text{wire } q} dl' J_z(l') \left[\frac{\partial G_i(l,l')}{\partial n'} + \frac{1}{2}\delta(l-l') \right] \quad (35)$$

where

$$G_i(\boldsymbol{\rho},\boldsymbol{\rho}') = \frac{i}{4} H_0^{(1)}\left(e^{i\pi/4} \sqrt{\omega\mu\sigma} \sqrt{(x-x')^2+(y-y')^2} \right) = \frac{1}{2\pi}\left[\ker \sqrt{\omega\mu\sigma} \sqrt{(x-x')^2+(y-y')^2} - i \operatorname{kei} \sqrt{\omega\mu\sigma} \sqrt{(x-x')^2+(y-y')^2} \right] \quad (36)$$

where "ker" and "kei" are the real and imaginary Kelvin functions. This equation applies to each wire separately; the range of integration is over the surface of that wire.

Using the boundary conditions (18) and (20) to eliminate A_z from the integral equation for the outside fields and add the condition on the total currents from (22),

$$\oint_{\text{all wires}} dl' G_o(l,l') \frac{\partial J_z(l')}{\partial n'} = \oint_{\text{all wires}} dl' \cdot \left[J_z(l') + i\omega\sigma A_q \right] \left[\frac{\partial G_o(l,l')}{\partial n'} - \frac{1}{2}\delta(l-l') \right] \quad (37)$$

$$\oint_{\text{wire } q} dl' G_i(l,l') \frac{\partial J_z(l')}{\partial n'} = \oint_{\text{wire } q} dl' J_z(l') \cdot \left[\frac{\partial G_i(l,l')}{\partial n'} + \frac{1}{2}\delta(l-l') \right] \quad (38)$$

$$\oint_{\text{wire } q} dl \frac{\partial J_z}{\partial n} = -\omega\mu\sigma I_q. \quad (39)$$

There is one important thing to note about these integral equations. Contrary to simpler electrostatic problems, the boundary conditions are neither Dirichlet nor Neumann; both G and $\partial G/\partial n'$ must be kept in the equations. Because of this, the formulation is in terms of the free-space Green's functions for Laplace's equation and the diffusion equation, (34) and (36). All information about the boundaries is contained in the paths of integration.

VI. Solution of Coupled Integral Equations

We solve these coupled integral equations, (37), (38), and (39), by the method of moments with subdomain basis functions. Expanding the unknown functions J_z and $\partial J_z/\partial n$ as the sum of known functions times unknown coefficients,

$$J_z = \sum_m j_m B_m(l) \quad (40)$$

$$\frac{\partial J_z}{\partial n} = \sum_m k_m B_m(l). \quad (41)$$

Simple pulse basis functions are used, normalized so that the integral is unity:

$$B_m(l) = \begin{cases} 1/\Delta_m & \text{if } l_m \leq l \leq l_m + \Delta_m \\ 0 & \text{otherwise.} \end{cases} \quad (42)$$

This gives a piecewise-constant approximation to the surface quantities. The same functions are used for testing, thereby implementing Galerkin's method.

It turns out that, for high frequencies, the current distribution on a wire is similar to the charge distribution on a perfect conductor. For polygonal wires, this means that the current will be concentrated at the corners. Therefore, we find it advantageous to concentrate the basis functions in the same way. For three basis functions on a side, for example, the two in the corners are each one eight the length of the side; the center one, three quarters. These values were determined empirically, by seeing which division gave results closest to those for a large number of basis functions.

We can thus approximate the coupled integral equation as a matrix equation:

$$\begin{bmatrix} \overline{\overline{V}}_o & \overline{\overline{W}}_o & \overline{\overline{U}}_o \\ \overline{\overline{S}} & 0 & 0 \\ \overline{\overline{V}}_i & 0 & \overline{\overline{U}}_i \end{bmatrix} \cdot \begin{bmatrix} \boldsymbol{K} \\ i\omega\sigma \boldsymbol{A}_o \\ \boldsymbol{J} \end{bmatrix} = \begin{bmatrix} 0 \\ -i\omega\mu\sigma \boldsymbol{I} \\ 0 \end{bmatrix} \quad (43)$$

where $\boldsymbol{J}$ is the vector of the unknown j_m's (current), $\boldsymbol{K}$ is the vector of the unknown k_m's (normal derivative of the current), and $\boldsymbol{A}_o$ is the vector of the A_q's (constants of vector potential). The total currents on each wire are specified by the vector $\boldsymbol{I}$. The matrices $\overline{\overline{V}}_o$, $\overline{\overline{W}}_o$, $\overline{\overline{U}}_o$, $\overline{\overline{S}}$, $\overline{\overline{V}}_i$, and $\overline{\overline{U}}_i$ arise from integrals of products of the Green's functions with the basis functions and are completely known. The solution of this matrix equation by LU decomposition provides us with an approximation for J_z and $\partial J_z/\partial n$, and through (25) and (27), R and L. Since the outer matrices $\overline{\overline{V}}_o$, $\overline{\overline{U}}_o$, $\overline{\overline{W}}_o$, and $\overline{\overline{S}}$, are independent of frequency, they only need to be calculated once. We can make use of this fact by LU-decomposing this part of the large matrix only once, completing the decomposition with the rest of the matrix for each value of frequency. For the pulse basis functions used, the outer matrices can

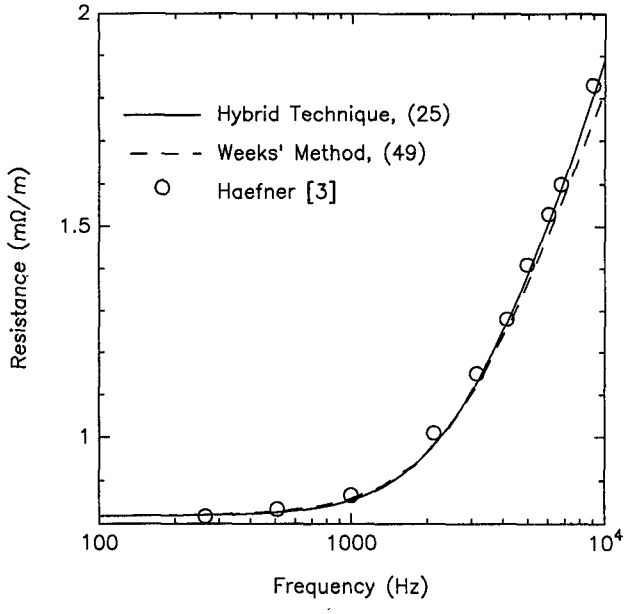

Fig. 2. Resistance of isolated square wire.

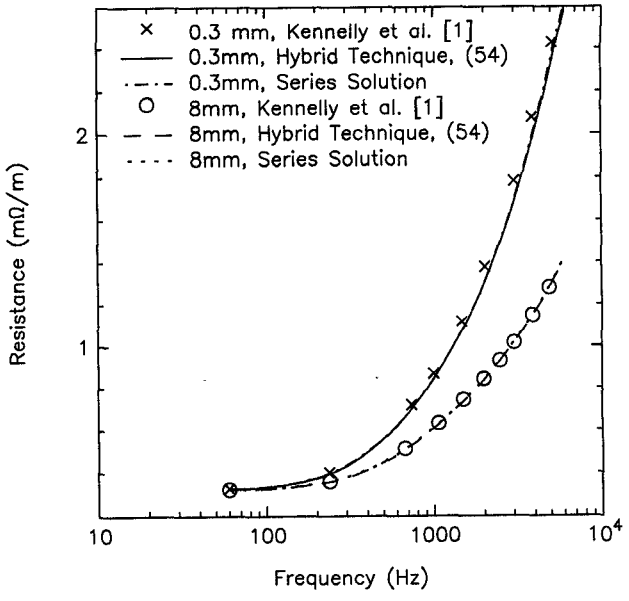

Fig. 3. Resistance of two circular wires.

be expressed in closed form. The inner matrices, $\bar{\bar{V}}_i$ and $\bar{\bar{U}}_i$, have, at worst, double numerical integrals, and for the case of the interaction between elements which lie on the same line, these can be expressed in closed form. Also, at high frequencies, owing to the highly local nature of the diffusion Green's function (36), which results from the rapidly decaying asymptotic nature of the Kelvin functions, only the neighboring patches have an appreciable interaction; those integrals can be calculated quite rapidly.

VII. Results

In these results, we will compare the hybrid method, described above, with experimental results, as well as with two other methods: the Weeks method [4], which models the current throughout the cross section, and the work of Djordjević *et al.* [23], which models an equivalent current only on the surface over all frequencies. As shall be seen, by using a hybrid method, we can avoid the weaknesses of both of these methods.

First, we consider the example of an isolated square conductor, 4.62 mm on a side, with conductivity $\sigma = 5.72 \times 10^7\ (\Omega - \mathrm{m})^{-1}$. While the inductance per unit length is undefined, the hybrid method can be used to calculate the resistance per unit length and for comparison with the experimental results of Haefner [3] and the results obtained by using the Weeks method [4]. As can be seen (Fig. 2), the fit for the new method is quite good. In this example, only 12 basis functions (25 unknowns) were used, three on a side. By comparison, the Weeks method with 49 basis functions does not give as good a result.

The next example is that of two parallel circular wires, $\sigma = 5.84 \times 10^7\ (\Omega - \mathrm{m})^{-1}$. The wires have a diameter of 11.68 mm, and a separation of 0.3 mm and 8 mm for the two cases. Here, the circles were modeled as n-sided polygons having the same cross-sectional area. In Figs. 3 and 4, the results for 13 basis functions per circle (54 unknowns) are shown, compared with the experimental results of Kennelly *et al.* [1]. The fit is again quite good with the experimental results. Since the Weeks method is limited to rectangular elements, it is not capable of handling this case.

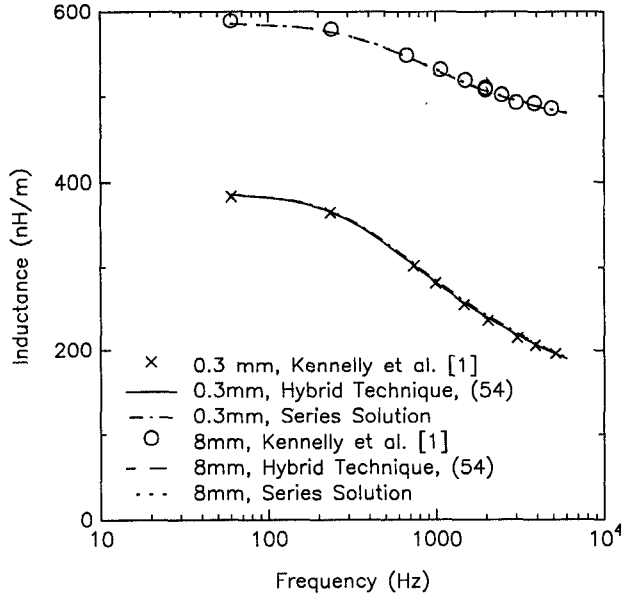

Fig. 4. Inductance of two circular wires.

Next, we take the example of two parallel rectangular wires, $\sigma = 5.6 \times 10^7\ (\Omega - \mathrm{m})^{-1}$; the configuration is shown in Fig. 5. In Figs. 6 and 7, we compare the hybrid method, the Weeks method, and the results from [23] calculated from a purely surface integral equation approach. It can be seen that the hybrid method agrees with each of the others in its range of validity. Also, the numerical instability of purely surface-integral equation methods in calcu-

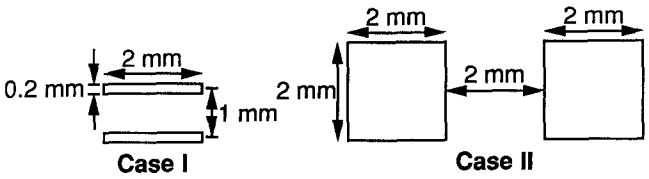

Fig. 5. Two rectangular wires.

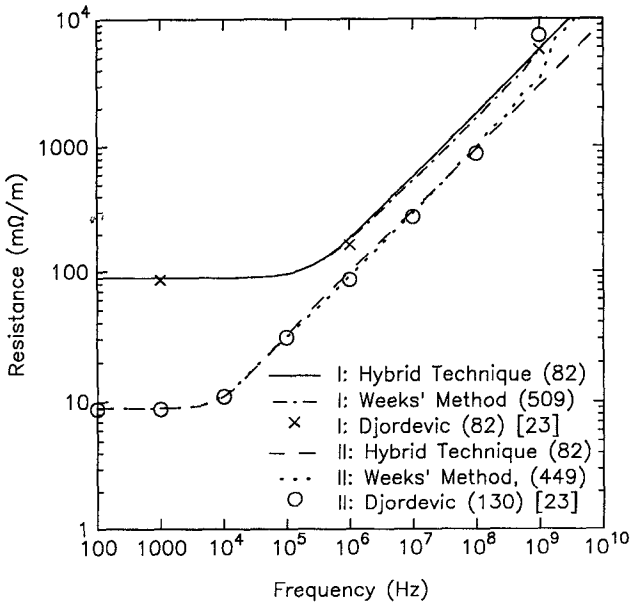

Fig. 6. Resistance of two rectangular wires.

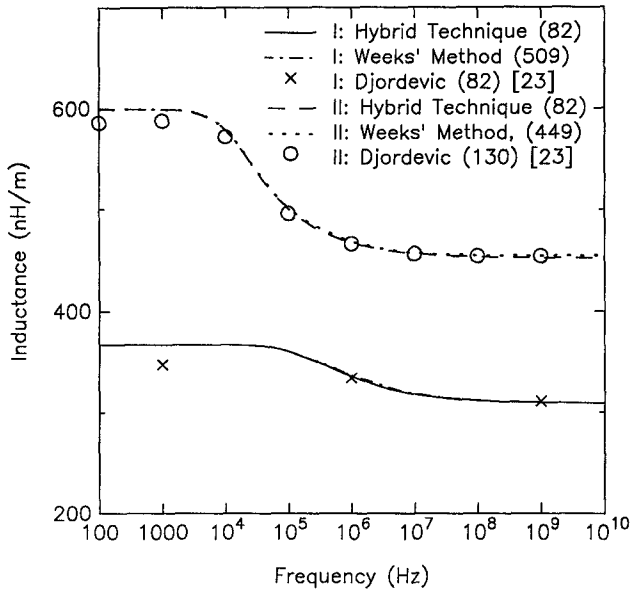

Fig. 7. Inductance of two rectangular wires.

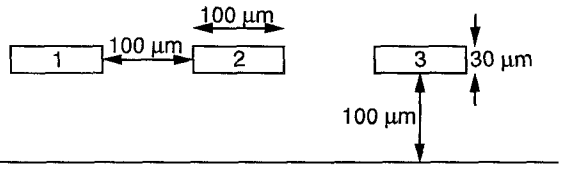

Fig. 8. Three rectangular wires over a ground plane.

lating the low-frequency inductance can be observed. It is also clear that the hybrid method in general requires fewer basis functions, and thus less computation time, than the Weeks method. In fact, as the frequency increases and the conductors become many skin depths across, even a large number of basis functions in the Weeks method leaves us with a significant error. This is due to the inability of the Weeks method to correctly model the distribution of current along the surface, which is crucial to the calculation of resistance at such frequencies. Tables I and II compare the results of the hybrid method with the Weeks method for the case of two square wires, including CPU times, on a Digital Equipment Corporation VAXstation 3500, running VMS. As can be seen, the cost of the hybrid method in terms of CPU time is much lower than the Weeks method for anything more than a moderate number of basis functions, and especially for high frequencies.

Finally, we consider the case of three rectangular conductors over a ground plane, $\sigma = 5.81 \times 10^7$ $(\Omega - \mathrm{m})^{-1}$. The configuration is shown in Fig. 8, the resistance of the first line in Fig. 9, and the self- and mutual inductances in Fig. 10. Since our method is not capable of modeling an infinite ground plane (since imaging is very difficult with an imperfect conductor), a very large conductor was used, 4 mm by 0.5 mm, in its place, with more basis functions concentrated in the area under the signal lines. We compare with the Weeks method and with a purely surface integral equation result, both with a large number of basis functions. The same trend can be seen as in the previous case, but there is now a large error in the high-frequency inductance, as predicted by the Weeks method. This is due to the fact that the Weeks method does not model the concentration of the current on the ground plane under the signal lines, since at high frequencies most of the patches are concentrated at the corners of the ground plane, far away from the current. If one improves the Weeks method by restricting the majority of basis functions to be under the signal lines, one gets results which agree with the hybrid method quite closely.

VIII. Conclusions

A technique has been developed to calculate the skin effect resistance and inductance of transmission lines with arbitrary cross sections. This technique provides accurate answers over a wide range of frequencies, including the range where neither low-frequency (direct current, uniform distribution) nor high-frequency (skin depth) approximations are valid. The technique is a hybridization of two distinct methods. The first is a cross-section coupled circuit approach, subdividing the wires into triangular patches which are assumed to have uniform current distribution. This method is best for low frequencies, when the physical current has very little variation across the cross section. The second method is in terms of a coupled integral equation, linking the current and its

TABLE I
RESULTS AND CPU TIMES FOR TWO SQUARE WIRES WITH HYBRID METHOD

Basis Functions	Number of Unknowns	Frequency (Hz)	R (mΩ/m)	L (nH/m)	CPU Time (s)
3×3	50		(Preprocessing)		12.99
		10^2	8.929	599.5	1.35
		10^4	11.07	577.7	3.36
		10^6	94.76	466.6	1.24
7×7	114		(Preprocessing)		19.16
		10^2	8.929	599.5	1.37
		10^4	11.13	579.6	17.00
		10^6	98.54	466.5	6.77
15×15	242		(Preprocessing)		155.79
		10^2	8.929	599.5	33.44
		10^4	11.15	580.2	156.49
		10^6	98.84	466.9	50.06

TABLE II
RESULTS AND CPU TIMES FOR TWO SQUARE WIRES WITH THE WEEKS METHOD

Basis Functions	Number of Unknowns	Frequency (Hz)	R (mΩ/m)	L (nH/m)	CPU Time (s)
3×3	17	10^2	8.929	599.5	0.76
		10^4	10.46	586.1	0.76
		10^6	118.8	466.9	0.75
7×7	97	10^2	8.929	599.5	50.14
		10^4	11.10	581.1	49.87
		10^6	92.60	468.5	49.43
15×15	449	10^2	8.929	599.5	3684.42
		10^4	11.22	580.1	3630.31
		10^6	91.80	468.1	3639.78

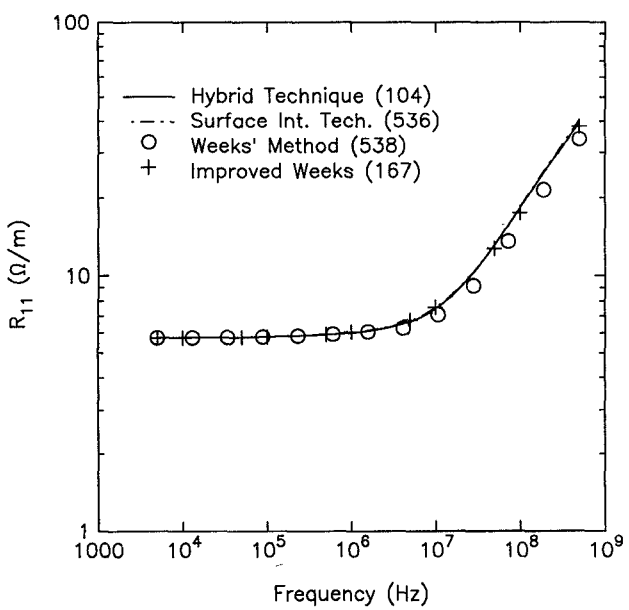

Fig. 9. Resistance of three rectangular wires over a ground plane.

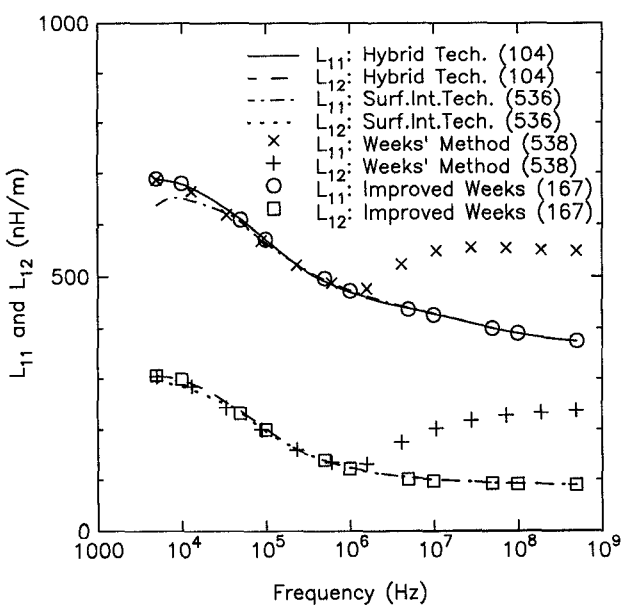

Fig. 10. Self- and mutual inductances of three rectangular wires over a ground plane.

normal derivative on the surface of each wire with the magnetic vector potential and its normal derivative on the same surfaces; the resistance and inductance are both expressed in terms of these surface quantities. This method is best for high frequencies, when the current is almost all confined to the surface, and the diffusion Green's function (eg. (36)) is very localized. For the middle frequency range, an interpolation between the two results gives very good accuracy with few basis functions. The interpolation function was based on the average size of the conductors, measured in skin depths, and was of the form $1/(1+0.16a^2/\delta^4)$, where a is the average cross section of the conductors, and δ is the skin depth. The optimization of the interpolation function is an area of

further research. By choosing triangular patches for the cross-section method and free-space Green's functions for the surface method, a single program is able to handle arbitrary conductors. The method is limited at present to infinite, uniform lines, although nothing theoretically prohibits extension to three-dimensional lines. The theory behind this method is not necessarily limited to configurations with uniform dielectrics, but problems in the definitions of resistance and inductance, stemming from difficulties with the extension of current and especially voltage to non-TEM lines, make such an extension of the method not immediately obvious. For most practical cases, however, the effects of nonuniform dielectrics on the resistance and inductance can be ignored, so that the method presented in this paper will give quick and accurate results.

Appendix
Closed-Form Expression for Partial Inductances

The problem is to evaluate the integral

$$I = \int\int dS_{ij} \int\int dS'_{km} \ln t \tag{A1}$$

where $t \equiv (x-x')^2 + (y-y')^2$ and the areas of integration are the triangular patches (ij) and (km). Using the fact that $\ln t = \nabla^2 \nabla'^2 t^2 (\ln t - 3)/64$, and Green's first identity (21)

$$I = \frac{1}{64} \oint dl_{ij} \oint dl'_{km} \frac{\partial}{\partial n} \frac{\partial}{\partial n'} \left[t^2 (\ln t - 3) \right] \tag{A2}$$

where the integrals dl_{ij} and dl'_{km} are over the perimeters of patches (ij) and (km), respectively, and the normals point out from the patches. Using the chain rule,

$$I = \frac{1}{32} \oint dl_{ij} \oint dl'_{km} \left[\frac{\partial^2 t}{\partial n \partial n'} t \left(\ln t - \frac{5}{2} \right) + \frac{\partial t}{\partial n} \frac{\partial t}{\partial n'} \left(\ln t - \frac{3}{2} \right) \right]. \tag{A3}$$

If the patches are polygons, these integrals over the perimeters of the wires become just sums of integrals over pairs of line segments. Therefore, we need to be able to evaluate this integral where the paths of integration are arbitrarily oriented line segments. Without loss of generality, the coordinate system is chosen so that the dl segment is parallel to the x axis (Fig. 11). In this case, the various derivatives of t are

$$t = (u + x_u - x_v - \cos\phi v)^2 + (y_u - y_v - \sin\phi v)^2 \tag{A4}$$

$$\frac{\partial t}{\partial n} = -\frac{\partial t}{\partial y_u} = 2(y_v - y_u + \sin\phi v) \tag{A5}$$

$$\frac{\partial t}{\partial n'} = -\cos\phi \frac{\partial t}{\partial y_v} + \sin\phi \frac{\partial t}{\partial x_v} = -2[\sin\phi(u - x_v + x_u) + \cos\phi(y_v - y_u) \tag{A6}$$

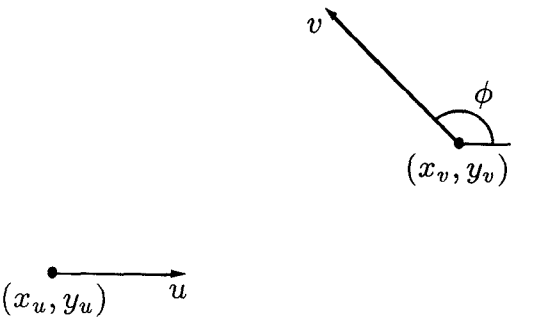

Fig. 11. Coordinate system for mutual inductance of triangular patches.

and

$$\frac{\partial^2 t}{\partial n \partial n'} = -\frac{\partial}{\partial y_u} \left(\frac{\partial t}{\partial n'} \right) = -2\cos\phi. \tag{A7}$$

Letting $x \equiv x_v - x_u$ and $y \equiv y_v - y_u$, the following double integral over the pair of line segments is obtained:

$$f(u,v) = \frac{1}{32} \int du \int dv\, t(5 - 2\ln t)\cos\phi + (6 - 4\ln t)(y + v\sin\phi) \cdot ((u-x)\sin\phi + y\cos\phi) \tag{A8}$$

where $t = (u - x - \cos\phi v)^2 + (y + \sin\phi v)^2$. These integrals can be done in closed form [25]. If the length of the dl segment is a, and that of the dl' segment is b, the contribution to (A1) from this pair of line segments is $f(a,b) - f(a,0) - f(0,b) + f(0,0)$. The total is thus the sum of the contributions from each pair of line segments, one from the (ij) patch and the other from the (km) patch.

References

[1] A. E. Kennelly, F. A. Laws, and P. H. Pierce, "Experimental researches on skin effect in conductors," *Trans. AIEE*, vol. 34-II, p. 1953, Sept. 1915.

[2] A. E. Kennelly and Affel, "Skin-effect resistance measurements of conductors at radio-frequencies up to 100,000 cycles per second," *Proc. IRE*, vol. 4, pp. 523–574, Dec. 1916.

[3] S. J. Haefner, "Alternating-current resistance of rectangular conductors," *Proc. IRE*, vol. 25, no. 4, pp. 434–447, Apr. 1937.

[4] W. T. Weeks, L. L. Wu, M. F. McAllister, and A. Singh, "Resistive and inductive skin effect in rectangular conductors," *IBM J. Res. Develop.*, vol. 23, no. 6, pp. 652–660, Nov. 1979.

[5] J. C. Maxwell, *A Treatise on Electricity and Magnetism*, vol. II. 1873, p. 291.

[6] W. Thomson, Lord Kelvin, *Mathematical and Physical Papers*, vol. 3, no. 102, pp. 484–515, 1889–1890.

[7] J. R. Carson, "Wave propagation over parallel wires: the proximity effect," *Phil. Mag.*, vol. 41, no. 24, pp. 607–633, Apr. 1921.

[8] J. D. Cockcroft, "Skin effect in rectangular conductors at high frequencies," *Proc. Roy. Soc.*, vol. 122, no. A-790, pp. 533–542, Feb. 1929.

[9] H. A. Wheeler, "Formulas for the skin-effect," *Proc. IRE*, vol. 30, pp. 412–424, Sept. 1942.

[10] H. B. G. Casimir and J. Ubbink, "The skin effect, I. Introduction; the current distribution for various configurations," *Philips Tech. Rev.*, vol. 28, no. 9, pp. 271–283, 1967.

[11] H. B. G. Casimir and J. Ubbink, "The skin effect, II. The skin effect at high frequencies," *Philips Tech. Rev.*, vol. 28, no. 10, pp. 300–315, 1967.

[12] P. Graneau, "Alternating and transient conduction currents in straight conductors of any cross-section," *Int. J. Electron.*, vol. 19, pp. 41–59, 1965.

[13] P. Silvester, "Modal network theory of skin effect in flat conductors." *Proc. IEEE*, vol. 54, no. 9, pp. 1147–1151, Sept. 1966.
[14] P. Silvester, "The accurate calculation of skin effect of complicated shape," *IEEE Trans. Power App. Syst.*, vol. PAS-87, pp. 735–742, Mar. 1968.
[15] A. Timotin, "Iteration method for study of the skin-effect in straight conductors," *Rev. Roum. Sci. Tech., Ser. Electrotech. Energ.*, vol. 10, no. 1, pp. 19–45, 1965.
[16] B. D. Popović and Z. D. Popović, "Method of determining power-frequency current distribution in cylindrical conductors," *Proc. Inst. Elec. Eng.*, vol. 119, no. 5, pp. 569–574, May 1972.
[17] P. Waldow and I. Wolff, "The skin-effect at high frequencies," *IEEE Trans. Microwave Theory Tech.*, vol. MTT-33, pp. 1076–1082, Oct. 1985.
[18] P. Waldow and I. Wolff, "Dual bounds variational formulation of skin effect problems," in *IEEE MTT-S Int. Microwave Symp. Dig.*, 1987, pp. 333–336.
[19] A. Konrad, "Integrodifferential finite element formulation of two-dimensional steady-state skin effect problems," *IEEE Trans. Magn.*, vol. MAG-18, pp. 284–292, Jan. 1982.
[20] G. Costache, "Finite-element solution of steady-state skin-effect problems in straight flat conductors," *COMPEL-Int. J. Comput. and Math. in Elec. and Electron. Eng.*, vol. 2, no. 2, pp. 35–39, 1983.
[21] G. Costache, "Finite element method applied to skin-effect problems in strip transmission lines," *IEEE Trans. Microwave Theory Tech.*, vol. MTT-35, pp. 1009–1013, Nov. 1987.
[22] A. C. Cangellaris, "The importance of skin-effect in microstrip lines at high frequencies," in *IEEE MTT-S Int. Microwave Symp. Dig.*, 1988, pp. 197–198.
[23] A. R. Djordjević, T. K. Sarkar, and S. M. Rao, "Analysis of finite conductivity cylindrical conductors excited by axially-independent TM electromagnetic field," *IEEE Trans. Microwave Theory Tech.*, vol. MTT-33, pp. 960–966, Oct. 1985.
[24] R.-B. Wu and J.-C. Yang, "Boundary integral equation formulation of skin effect problems in multiconductor transmission lines," *IEEE Trans. Magn.*, vol. MAG-25, pp. 3013–3015, July 1989.
[25] M. J. Tsuk, "Propagation and interference in lossy microelectronic integrated circuits," Ph. D. thesis, Department of Electrical Engineering and Computer Science, Massachusetts Institute of Technology, June 1990.

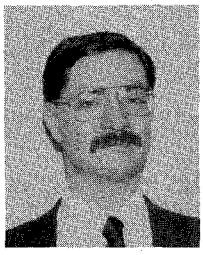

Michael J. Tsuk was born in Yonkers, NY, on January 24, 1964. He received the S.B., S.M., and Ph.D. degrees in electrical engineering from the Massachusetts Institute of Technology in 1984, 1986, and 1990, respectively.

Since 1990, he has been with the Physical Technology Group of the Digital Equipment Corporation, Andover, MA. He is an Assistant Editor for the *Journal of Electromagnetic Waves and Applications* (*JEWA*). His research interests include time-domain electromagnetics and numerical methods for the design of high-performance integrated circuit packaging.

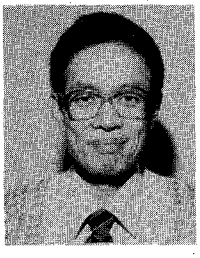

Jin Au Kong (S'65–M'69–SM'74–F'85) is Professor of Electrical Engineering and Chairman of Area IV and Energy and Electromagnetic Systems in the Department of Electrical Engineering and Computer Science at the Massachusetts Institute of Technology, Cambridge, MA. From 1977 to 1980 he served the United Nations as a High-Level Consultant to the Under-Secretary-General on Science and Technology, and as an Interregional Advisor on remote sensing technology for the Department of Technical Cooperation for Development. His research interests are in the area of electromagnetic wave theory and applications. He has published six books and more than 300 refereed journal and conference papers and has supervised more than 100 theses.

Dr. Kong is the Editor for the Wiley series on remote sensing, the Editor-in-chief of the *Journal of Electromagnetic Waves and Applications* (*JEWA*), and the Chief Editor for the Elsevier book series on Progress in Electromagnetics Research (PIER).